Polarity of GaN nanowires grown by plasma-assisted molecular beam epitaxy on Si(111)

Karine Hestroffer,[1,*] Cédric Leclere,[2] Catherine Bougerol,[3] Hubert Renevier,[2] and Bruno Daudin[1]
[1]*CEA-CNRS group "Nanophysique et Semiconducteurs," Université Joseph Fourier and CEA Grenoble, INAC, SP2M, 17 rue des Martyrs, 38 054 Grenoble, France*
[2]*Laboratoire des Matériaux et du Génie Physique, Grenoble INP - MINATEC, 3 parvis L. Néel 38016 Grenoble, France*
[3]*CEA-CNRS group "Nanophysique et Semiconducteurs," Institut Néel, CNRS and Université Joseph Fourier, BP 166, F-38042 Grenoble Cedex 9, France*
(Received 11 August 2011; published 7 December 2011)

Based on the breakdown of Friedel's law, resonant x-ray diffraction is shown to be a suitable method to determine polarity of non-centrosymmetrical wurtzite gallium nitride (GaN) nanowires (NWs) at a macroscopic scale. It is demonstrated that such GaN NWs grown by plasma-assisted molecular beam epitaxy on bare Si(111) are N-polar, consistent with results obtained by convergent beam electron diffraction. The N-polarity feature is attributed to the formation of a thin Si_xN_{1-x} layer on the Si surface before growth. The use of a thin AlN buffer layer does not modify the GaN NW polarities, suggesting that NWs actually grow between the AlN grains rather than on top of them.

DOI: 10.1103/PhysRevB.84.245302 PACS number(s): 61.46.Km, 61.05.cp

I. INTRODUCTION

Polarity is an intrinsic property of non-centrosymmetrical crystalline structures such as wurtzite. The lack of center of symmetry may induce a spontaneous polarization within the cell, leading to the presence of an internal electrical field, the amplitude of which directly depends on the relative positioning of the atoms in the unit cell and therefore on the lattice parameters. Furthermore, strains within the structure produce an additional piezoelectric polarization that contributes to the total electric field. In the case of heterostructures, the discontinuity of the electric field raising from the difference of polarization between the two materials may lead to the formation of two-dimensional (2D) electron gases at the interfaces. In the case of quantum wells embedded in a barrier material, this gives rise to a carrier separation responsible for a red shift of the luminescence and a reduction of the oscillator strength. This drawback for optical properties, known as quantum confined stark effect (QCSE), has been extensively investigated in III-N semiconductor heterostructures, which are of great interest for optoelectronic applications in the large range of wavelengths covered by the different III-N alloys spanning over the whole visible spectrum down to UV. Nevertheless, considering the lack of appropriate substrates, the growth of high structural quality, defect-free III-N layered heterostructures is difficult. An alternative to this issue has appeared with the breakthrough of gallium nitride nanowires (GaN NWs) grown by plasma-assisted molecular beam epitaxy (PAMBE) on sapphire or silicon[1,2] since no epitaxial relation to the substrate is necessary. With the recent mastering of selective area growth,[3] GaN NWs moreover appear as an attractive base for localized heterostructures such as InGaN on GaN NWs,[4,5] GaN/AlN core-shell NWs,[6] or GaN/AlN quantum dots (QDs) in GaN NWs.[7] It has been demonstrated that, in the case of such GaN QDs, although the piezoelectric component is reduced because of an efficient strain relaxation allowed by the NW geometry, QCSE is still significant, leading to a red shift of the GaN QD emission. Based on a tight-binding method, it has been shown that such an electric field is screened to a large extent by the charges pulled out from the top of the NW heterostructures.[8] This mechanism, crucial to prediction of the optical properties of NW heterostructures is polarity dependent. In the case of 2D layers, it has been found that polarity influences the morphology of the surface, the crystal quality,[9–11] and, most importantly, the incorporation of impurities and vacancies during growth[12] that itself critically affects the optical properties. It is reasonable to expect similar features in the case of NWs, emphasizing the necessity for an absolute determination of their chemical termination, namely metal or N, to fully understand their optical properties.

When speaking of polarity, one usually refers to the direction along which GaN grows by considering the Ga-N bond that is colinear to the c-axis of the wurtzite cell. The vector going from Ga and pointing toward N conventionally defines [0001], the positive direction of the c-axis. A structure is said to be Ga-polar or Ga-terminated when its growth direction is [0001]. Reciprocally, a structure is said to be N-polar when its growth direction is $[000\bar{1}]$. A large panel of experimental methods such as ion channeling, hemispherically scanned x-ray photoelectron diffraction, x-ray standing wave, Auger electron spectroscopy or coaxial impact-collision ion scattering spectroscopy may be used to determine the polarity of thick 2D layers. In the case of GaN, it has been already widely investigated[9,11,13–16] and appears to depend on the growth technique (metalorganic chemical vapor deposition or MBE), the substrate [Sapphire, Si(111), SiC(0001)], the use or not of a buffer layer, and the growth conditions, leading to a wide set of sometimes contradictory experimental results in literature.[17]

Regarding layers grown by PAMBE on sapphire, polarity is determined by the surface nitridation temperature prior to growth[11] or can be controlled by tuning the polarity of an AlN buffer layer, itself determined by the Al/N ratio during deposition.[18] Interestingly, N-polar GaN layers have also been grown successfully on Si_3N_4/Si(111).[19] More recently, studies have been performed on GaN wires with a diameter in the range of 1–5 μm, grown by metalorganic vapor phase epitaxy or amonia-MBE.[20,21] Wires grown on nitrided c-sapphire substrate exhibit a mixture of Ga- and N-polarity with a tendency to be rather N-polar while wires grown on Si(111) appear to be Ga-polar at 90%. However, in what concerns the

polarity of PAMBE GaN NWs, literature is rather poor and does not lead to clear conclusions.[22–25]

In such an open context, the prospect of this work is to present a reliable, diameter-independent method to determine the polarity of PAMBE GaN NWs, which is based on the use of resonant effects in x-ray diffraction (XRD).[26–31] We show that the polarity of GaN NWs grown by PAMBE on bare Si(111) is N, consistent with the results suggested by convergent-beam electron diffraction (CBED). It has also been determined that KOH selectively etches NW N-polar sides, allowing us to verify the polarity of GaN NWs grown in various conditions.

II. SAMPLE PREPARATION

A reference sample was grown by PAMBE on a 2-inch Si(111) substrate previously deoxidized by HF (5%) and outgassed until the appearance of a 7×7 surface reconstruction. GaN NWs were then grown directly on Si at a temperature of 800 °C in the usual N-rich conditions with a III/V flux ratio of 0.4. Importantly, growth was initiated by simultaneously opening the Ga and the N shutter. By the end of the 3.5 h growth period, as-grown NWs (a-NWs) were 730 nm long and had a diameter of 30 nm on average and a density of about 200 NWs/μm^2.

To prepare a sample with upended NWs (u-NWs), a 5-mm^2 piece was cleaved from the center of the Si wafer and stuck upside down onto a sapphire lump with heated pine resine. When cooled, the pine resin hardened, ensuring the formation of a resistant Al_2O_3/GaN NW/Si stack. Next, this sandwich-like assembly was plunged for several hours into a solution of 10 mL of hydrofluoric acid (49%), 10 mL of nitric acid (65%), and 30 mL of acetic acid (100%). This chemical solution selectively etched the Si, leaving the u-NWs embedded in the pine resin on top of the untouched sapphire.

III. EXPERIMENTAL DETAILS AND RESULTS

A. Transmission electron microscopy study

CBED patterns were then recorded for a few NWs of the a-NW sample prepared in cross section and observed along the [10-10] zone axis. The experiment was carried out on a FEI-Titan microscope operated at 200 kV. The asymmetry between the 0002 and 000-2 reflections enabled us to assign the polarity of the NWs by comparing experimental data with computer simulations performed with the JEMS software (Fig. 1). We determined in this way that the a-NWs were N-polar. However, even though the results appeared convincing, we faced several limitations during this study: first, we could not record patterns for significantly different thicknesses (a method commonly used for CBED studies) because of the rather good homogeneity in size of the NWs; moreover, the features inside the disks for small thicknesses (about 30 nm) are rather faint. Additionally, the NWs were often slightly bent because of the glue around them (cross-section preparation) which made the precise orientation quite tricky. Finally, it must be pointed out that CBED is a microscopic method, giving information on individual NWs but not on the whole population.

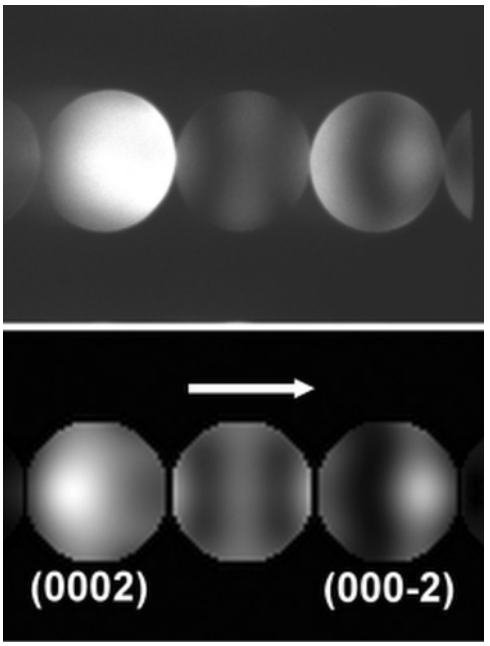

FIG. 1. Experimental (top) and simulated (bottom) CBED patterns for 30-nm-thick a-NWs sample at 200 kV. The growth direction is represented by the white arrow.

B. X-ray diffraction investigation

For these reasons, resonant XRD was used to determine GaN NW polarity unambiguously and at a macroscopic scale. This approach is based on the well-known breakdown of Friedel's law—demonstrated for the first time in the 1930s for wurtzite ZnS structure[26,27]—a disparity in the diffracted intensity of Bijvoet pairs of reflections that occurs for noncentrosymmetrical systems when resonant effects are no longer negligible.[32] Friedel pairs refer to reflections with Miller indices hkl and $\overline{hkl}$, whereas Bijvoet pairs refer to reflections symmetrically equivalent to hkl and $\overline{hkl}$ reflections.

The intensity $I(hkl)$ of the diffracted x-ray beam is proportional to the square of the complex structure factor $F(hkl)$, which can be expressed as[33]

$$F(hkl) = F_{\mathrm{T}}(hkl) + F'_{\mathrm{A}}(hkl) + i\,F''_{\mathrm{A}}(hkl), \qquad (1)$$

where $F_{\mathrm{T}}(hkl)$ includes the Thomson scattering of all atoms and the anomalous scattering of non resonant atoms (i.e., the nonresonant contribution of all species). $F'_{\mathrm{A}}(hkl) + i\,F''_{\mathrm{A}}(hkl)$ is the complex anomalous scattering factor corresponding to the scattering contribution of all resonant atoms A, $F'_{\mathrm{A}}(hkl)$ and $F''_{\mathrm{A}}(hkl)$ being related respectively to dispersion and absorption. It can be seen from the Argand diagram in Fig. 2 that $F''_{\mathrm{A}}(hkl)$, the absorption part of the resonant contributions, introduces a $\frac{\pi}{2}$ phase shift that induces a difference in the magnitude of the two total structure factors $F(hkl)$ and $F(\overline{hkl})$. As a consequence, the two reflections hkl and $\overline{hkl}$ diffract with distinct intensities that allow their strict identification, and thus the determination of the crystal orientation. Using the as-grown sample, we could therefore deduce the NW growth direction—hence, GaN NW polarity. Complementally, the u-NWs were used to assert the polarity of the opposite direction. Let us note here that the use of u-NWs is justified by

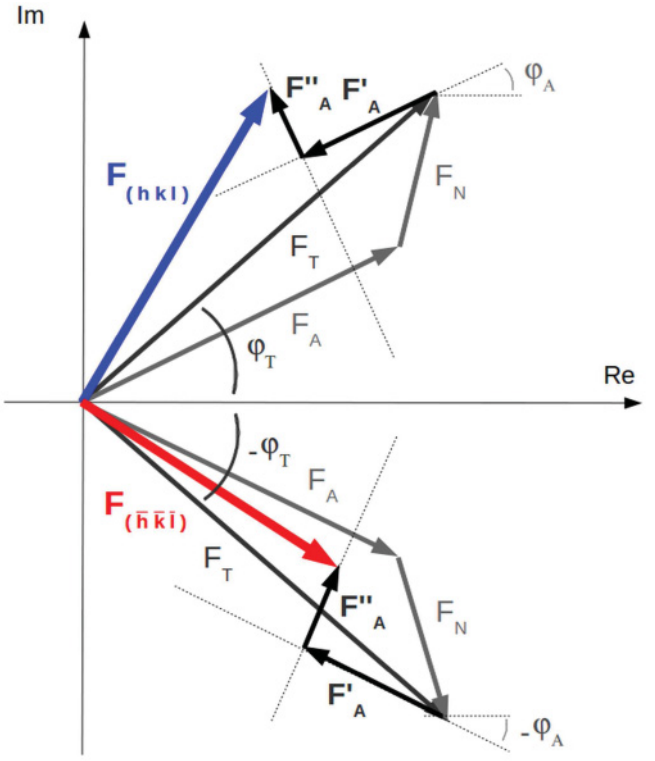

FIG. 2. (Color online) Argand diagram illustrating the breakdown of Friedel's law: a difference in the magnitude of the two total structure factor $|F(hkl)|$ and $|F(\overline{hkl})|$ moduli (thus in the diffracted intensity) occurs for non-centrosymmetrical systems when the absorption term F''_A of the resonant dispersive corrections is involved. F_T is the structure factor that includes the Thomson scattering of all atoms and the anomalous scattering of all nonresonant atoms (i.e., $F_T = F_A + F_N$ where F_A corresponds to the Thomson scattering of all resonant atoms, and F_N gathers both Thomson and anomalous contributions of nonresonant atoms (nitrogen atoms in this study). $F'_A(hkl) + iF''_A(hkl)$ is the complex anomalous scattering of all resonant atoms (Ga atoms in the present study), $F'_A(hkl)$ and $F''_A(hkl)$ are related to dispersion and absorption, respectively.

the impossibility of reaching the second reflection of the pair through the highly absorbent 250-μm-thick Si substrate.

X-ray diffraction experiments with monochromatic synchrotron radiation were carried out at the beamline BM02/D2AM at the European Synchrotron Radiation Facility (ESRF). Intensity of symmetric Bragg reflections were measured with an eight-circle diffractometer (Euler geometry). Beam size at the focal point was about 0.3 × 0.15 mm^2, thus illuminating a large assembly of NWs. Based on calculations, the difference in intensity between the 112 and $\bar{1}\bar{1}2$ (or $11\bar{2}2$ and $\bar{1}\bar{1}2\bar{2}$ in the four-index notation) strong reflections appeared to be significant enough, accounting for our choice to use this Bijvoet pair for the experiment. To thoroughly highlight the experimental intensity difference, extended and precise scans in energy around the Ga K-edge (10367 eV) were recorded. The background intensity was additionally monitored to correct the data for fluorescence and diffuse scattering signals. For each Bijvoet pair reflection, we measured and averaged three intensity spectra (5 seconds per point each). Background-subtracted data are displayed in

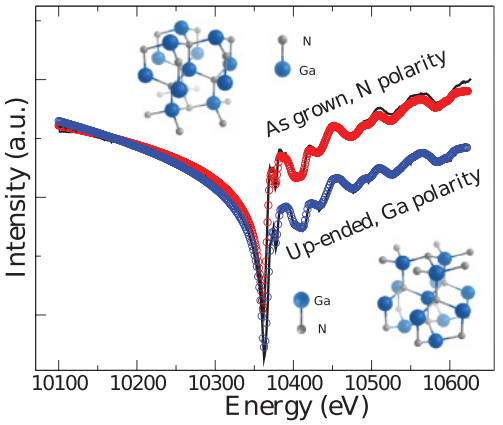

FIG. 3. (Color online) Evolution of the intensity of the $(11\bar{2}2)$ and $(\bar{1}\bar{1}2\bar{2})$ pair with the energy around the Ga K-edge. Because of the non-centrosymmetrical characteristic of the wurtzite GaN structure, a discrepancy in intensity is clearly observed. In this way, a-NWs and u-NWs are identified as N-polar and Ga-polar, respectively.

Fig. 3 and exhibit a clear difference in intensity close to and after the Ga K-edge. The experimental error is estimated to be 1–2% for the averaged intensities, which is included in the circles in Fig. 3.

Following multiwavelength anomalous diffraction formalism,[33] the structure factor $F(hkl)$ corresponds to

$$F(hkl,E) = F_T(hkl) + \frac{F_A(hkl)}{f_A^0}[f'_A(E) + if''_A(E)]. \quad (2)$$

Therefore, the diffracted intensity is proportional to

$$|F(hkl,E)|^2 = \left[|F_T|\cos(\varphi_T - \varphi_A) + \frac{|F_A|}{f_A^0}f'_A\right]^2 + \left[|F_T|\sin(\varphi_T - \varphi_A) + \frac{|F_A|}{f_A^0}f''_A\right]^2, \quad (3)$$

where φ_T and $\varphi_A = 2\pi\sum_{j=1}^{N_A} hx_j + ky_j + lz_j$ are the phases of the complex structure factors F_T and F_A, respectively. In Eq. (3), structure factor moduli do not depend on whether $h,k,l = 1,1,2$ or $\bar{1},\bar{1},\bar{2}$, but the phase difference $\varphi_T - \varphi_A$ does. As a matter of fact, if one neglects the anomalous scattering contributions of nonresonant atoms (N atoms), then the phase differences $\varphi_T - \varphi_A$ for $11\bar{2}2$ and $\bar{1}\bar{1}2\bar{2}$ reflections are of opposite sign. Thomson scattering factors were calculated with the parameterized formula of D. Waasmaier and A. Kirfel.[35] Resonant scattering factors f'_A and f''_A were obtained two ways. For nitrogen atoms, we used the theoretical value obtained with the Cromer and Liberman program.[36] On the other hand, for resonant gallium atoms, f''_A were obtained by rescaling the fluorescence data (multiplied by the incoming beam energy) of the sample to theoretical f''_A values, whereas f'_A were calculated from experimental f''_A by using the Kramers–Kronig transforms.[32] To calculate these f'_A values, we used a difference Kramers–Kronig method implemented in the DIFFKK software.[37]

The measured diffracted intensity is $I(hkl) = KD(E)I_0\lambda^3 LPA|F(hkl)|^2$, where K is a scale factor, $D(E)$ is the detector efficiency, I_0 is the intensity of the incident x-ray beam,

λ is the x-ray wavelength, L and P are the Lorentz and polarization factors, respectively, and A is the absorption factor. We assumed that L and P are the same for each reflection of the Bijvoet pair, being independent of the x-ray beam energy and not contributing to the difference in intensity. The absorption term A does depend on the energy, but the effect is rather weak compared with the anomalous one. To take into account the self-absorption that reduces the diffracted intensity by about 5–10%, we applied an absorption correction to theoretical spectra for symmetric Bragg geometry. A was calculated from the following formula given for a thin film of thickness τ,[34]

$$A(hkl,E) = \frac{1}{\sin(\alpha)} \int_0^{\tau} \exp(-2\mu z/\sin\alpha) dz = \frac{1-\exp(-2\mu\tau/\sin\alpha)}{2\mu}, \quad (4)$$

where α is the incident angle and μ is the linear absorption coefficient. The absorption correction takes into account the change of the x-ray beam footprint area as a function of α. For reflections $11\bar{2}2$ and $\bar{1}\bar{1}2\bar{2}$ measured in symmetric Bragg condition, incident and exit angles value are equal to $\alpha = 14^\circ$ in the energy range of 10 150–10 650 eV. τ is the thickness of the film. In the case of NWs, we used τ_{eq}, an equivalent thickness defined by $\tau_{eq} = L \times \pi(D/2)^2 \times S =$ 150 nm, where L, D, and S are the length, diameter, and surface density, respectively, of the NWs as determined by scanning electron micrographs.

Finally, Eq. (2) was used to fit the background-subtracted spectrum with a Levenberg–Marquandt algorithm given by the SciPy.optimize (version 0.7.0) package. Only geometrical parameters [scale factor K and $D(E)$] were fitted. Experimental data obtained from the a- and u-NW samples, as well as the best fits (solid lines), are shown in Fig. 3. One can clearly identify the a-NWs as N-polar and the u-NWs as Ga-polar. The macroscopic size of the beam area hitting the sample, together with the excellent agreement between fit and experimental data, clearly excludes the contingency of polarity mixing.

C. KOH etching test

As a complementary experiment, one piece of the a-NW sample was then plunged into a solution saturated with KOH for 10 minutes at room temperature. In the case of 2D GaN layers, it is known that KOH selectively etches N-polar surfaces, leaving the Ga-polar ones untouched.[10] However, to our knowledge, in the case of NWs, no exhaustive investigation has been performed so far: one can wonder how KOH acts on nonpolar facets, such as those exhibited by GaN NWs inherent to their geometry. It was therefore relevant to ascertain that, similar to the 2D case, the NW N-polar face was etched in a pencil-like shape [Fig. 4(a) and 4(b)]. Concerning the effect of KOH on the NW Ga-polar face, the u-NW sample appeared to be inconvenient because of the residual pine resin remaining between the NWs, making the growth of a specific sample necessary. In this sample, to identify the top from the bottom of the NWs, a thin AlN section was inserted near the top of the NWs. Figure 4(c) shows a scanning electron micrograph taken in transmission of such a NW heterostructure after the NWs were dispersed onto a cooper grid covered with a carbon membrane. The carbon grid was then plunged into the KOH solution, therefore exposing both N- and Ga-polar sides of the NWs to the etchant. In Fig. 4(d), it is clear that the top part of the NWs (identified by the position of the AlN insertion) is etched, whereas the bottom part remains flat. As in the case of 2D layers, the KOH therefore selectively etches the NW N-polar sides while leaving untouched their Ga-polar face,

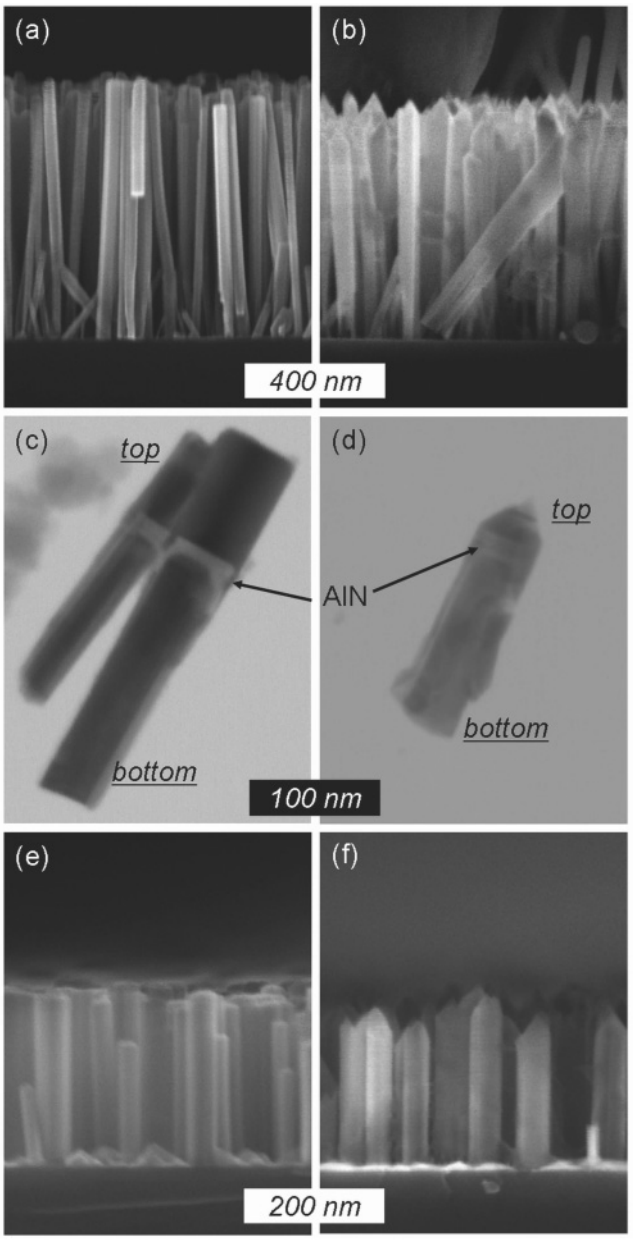

FIG. 4. Side-view scanning electron micrographs (SEM) of NWs on their original substrate (a, b, e, f) and SEM in transmission images of GaN NWs containing a thin AlN insertion near their top (c, d). The flat top surface of N-polar NWs grown on bare Si(111) (a, c) is etched into a pencil-like shape after being dipped for 10 minutes in a solution saturated with KOH (b, d). The Ga-polar side (i.e., the bottom of N-polar NWs) (c) remains flat after being plunged into the same bath (d). GaN NWs grown on a thin AlN buffer layer (e) are also etched by KOH (f), a signature of their N-polar character.

evidence that KOH selective etching can be valuable as a quick method to evaluate the polarity of GaN NWs.

IV. DISCUSSION

In the case of 2D GaN layers deposited by PAMBE on Si(111), it has been established that direct growth leads to N-polarity, whereas the use of a thin AlN buffer layer on Si(111) results in Ga-polar GaN layers. Moreover, the N-polarity character of the layer has been assigned to the formation of a Si_xN_{1-x} layer at the interface between Si and GaN.[19] Indeed, at the usual NW growth temperature (i.e., in the 800 °C range), Si is found to be dissolved when exposed to Ga.[38,39] However, the N-rich conditions and the strong reactivity of N with Si favor a nitridation of the Si surface at the very beginning of GaN growth. In the case of PAMBE growth of GaN NWs, nitridation of the Si surface systematically occurs when turning on the plasma cell before growth: it has been found that depending on the shutter technology, a leakage of active nitrogen that may nitridate the surface is likely taking place.[23] This unavoidable feature presumably leads to the formation of a thin Si_xN_{1-x} layer on the Si surface before the start of growth.[40] To avoid this unintentional nitridation, an attempt to protect the Si(111) surface was made by leaving the substrate under a constant Ga flux before starting NW growth. Although direct exposure of the surface to nitrogen was avoided, NWs still exhibited N-polarity, as checked by the KOH etching method, consistent with the preferential formation of Si-N bounds when exposing a Si(111) surface to both N and Ga.[19]

An additional sample was prepared with GaN NWs grown on a 2–3-nm-thick AlN buffer layer on Si(111). The AlN buffer layer was grown by supplying Al and N alternately. GaN NWs grown in similar conditions as those described above positively reacted to KOH etching [Fig. 4(e) and 4(f)], revealing N-polarity. Interestingly, AlN grown on Si(111) has been shown to be Al-polar,[41] which should result in the formation of Ga-polar GaN NWs. The apparent contradiction between this statement and the evidence of N-polarity for GaN NWs grown on a thin AlN buffer layer may be overcome by considering that GaN NWs/AlN/Si(111) actually grow on the edge of the grains of the buffer layer[42] and not on top of it, consistent with results obtained on sapphire by Sekiguchi *et al.*[43] Additionally, it has also been established by both groups that NW growth was inhibited for an AlN buffer layer thicker than a critical thickness of several nanometers. This strongly suggests that GaN NW nucleation is initiated on the Si surface between the grains of the AlN buffer layer. It also suggests that the absence of in-plane mosaicity observed when growing GaN NWs on Si(111) using a thin AlN buffer layer is not related to the nucleation itself but rather to an epitaxial relationship of growing GaN NWs on the adjacent buffer grains.[44,45] Such a hypothesis is supported by the evidence that AlN, despite its large mismatch with Si(111), actually grows in epitaxy onto it, because of a coincident relationship at the interface.[46]

Furthermore, the N-polar character of GaN NWs is in agreement with theoretical predictions about the presence of QCSE in GaN NW heterostructures.[8] It has been indeed shown that the pyroelectric field pulls out charges from the top surface of the NWs, which accumulate below the heterostructures and screen the spontaneous polarization. In Ga-face NWs, the pyroelectric field leaves positive charges at the top surface (emptied surface states first, then valence band holes), whereas in N-face NWs, it leaves negative charges (filled surface states, then conduction band electrons). The magnitude of the experimental electric field suggests that the Fermi level lies near or in the valence band at the top of Ga-polar NWs and in the conduction band in N-polar NWs. Given the experimental evidence that the Fermi level tends to be pinned close to the conduction band in nitride materials (presumably because of oxygen defects), N-face NWs are more consistent with the experimental values of the electric field.[8]

V. CONCLUSION

Resonant XRD was shown to be a suitable method to determine GaN NW polarity at a macroscopic scale. We established that GaN NWs grown on bare Si (111) by PAMBE are entirely N-polar, consistent with what was observed by CBED for few NWs. The N-polarity character is believed to be a consequence of the formation of a thin Si_xN_{1-x} layer on the Si surface prior to or at the beginning of GaN growth because of the strong Si-N affinity. GaN NWs grown on a thin AlN buffer layer on Si(111) likewise exhibited N-polarity, supporting the hypothesis of a nucleation between the AlN grains rather than on top of it.

ACKNOWLEDGMENTS

The authors thank the French CRG at the ESRF for allocating beamtime, as well as the BM02 staff (S. Arnaud, J. F. Bérar, N. Boudet, B. Caillot) for their help during the experiments. This work is supported by French National Agency (ANR) through the Nanoscience and Nanotechnology Program (Project BONAFO n°ANR-08-NANO-031-01).

*karine.hestroffer@cea.fr

[1] M. A. Sanchez-Garcia, E. Calleja, E. Monroy, F. J. Sanchez, F. Calle, E. Muñoz, and R. Beresford, J. Cryst. Growth **183**, 23 (1998).

[2] M. Yoshizawa, A. Kikuchi, M. Mori, N. Fujita, and K. Kishino, Jpn. J. Appl. Phys. **36**, L459 (1997).

[3] K. Kishino, T. Hoshino, S. Ishizawa, and A. Kikuchi, Electron. Lett. **44**, 13 (2008).

[4] G. Tourbot, C. Bougerol, A. Grenier, M. Den Hertog, D. Sam-Giao, D. Cooper, P. Gilet, B. Gayral, and B. Daudin, Nanotechnology **22**, 075601 (2011).

[5] F. Limbach, T. Gotschke, T. Stoica, R. Calarco, E. Sutter, J. Ciston, R. Cusco, L. Artus, S. Kremling, S. Höfling, L. Worschech, and D. Grützmacher, J. Appl. Phys. **109**, 014309 (2011).

[6] K. Hestroffer, R. Mata, D. Camacho, C. Leclere, G. Tourbot, Y. M. Niquet, A. Cros, C. Bougerol, H. Renevier, and B. Daudin, Nanotechnology **21**, 415702 (2010).

[7] J. Renard, R. Songmuang, G. Tourbot, C. Bougerol, B. Daudin, and B. Gayral, Phys. Rev. B **80**, 121305 (2009).

[8] D. Camacho Mojica and Y. M. Niquet, Phys. Rev. B **81**, 195313 (2010).

[9]M. Seelmann-Eggebert, J. L. Weyher, H. Obloh, H. Zimmermann, A. Rar, and S. Porowski, Appl. Phys. Lett. **71**, 2635 (1997).
[10]L. Dongsheng, M. Sumiya, K. Yoshimura, Y. Suzuki, Y. Fukuda, and S. Fuke, Phys. Status Solidi A **180**, 357 (2000).
[11]A. Georgakilas, S. Mikroulis, V. Cimalla, M. Zervos, A. Kostopoulos, Ph. Komninou, Th. Kehagias, and Th. Karakostas, Phys. Status Solidi A **188**, 567 (2001).
[12]S. F. Chichibu, A. Setogucchi, A. Uedono, K. Yoshimura, and M. Sumiya, Appl. Phys. Lett. **78**, 28 (2001).
[13]B. Daudin, J. L. Rouvière, and M. Arlery, Appl. Phys. Lett. **69**, 2480 (1996).
[14]A. R. Smith, R. M. Feenstra, D. W. Greve, M.-S. Shin, M. Skowronski, J. Neugebauer, and J. E. Northrup, Appl. Phys. Lett. **72**, 2114 (1998).
[15]A. Kazimirov, G. Scherb, J. Zegenhagen, T.-L. Lee, M. J. Bedzyk, M. K. Kelly, H. Angerer, and O. Ambacher, J. Appl. Phys. **84**, 1703 (1998).
[16]A. Yoshikawa and K. Xu, Thin Solid Films **412**, 38 (2002).
[17]M. Sumiya and S. Fuke, MRS Internet J. Nitride Semicond. Res. **9**, 1 (2004).
[18]X. Wang and A. Yoshikawa, Prog. Cryst. Growth Charact. Mater. **48**/**49**, 42 (2004).
[19]S. Gangopadhyay, T. Schmidt, and J. Falta, Phys. Status Solidi B **243**, 1416 (2006).
[20]X. J. Chen, G. Perillat-Merceroz, D. Sam-Giao, C. Durand, and J. Eymery, Appl. Phys. Lett. **97**, 151909 (2010).
[21]B. Alloing, S. Vézian, O. Tottereau, P. Vennéguès, E. Beraudo, and J. Zuniga-Pérez, Appl. Phys. Lett. **98**, 011914 (2011).
[22]D. Cherns, L. Meshi, I. Griffiths, S. Khongphetsak, S. V. Novikov, N. Farley, R. P. Campion, and C. T. Foxon, Appl. Phys. Lett. **92**, 121902 (2008).
[23]F. Furtmayr, M. Vielemeyer, M. Stutzmann, J. Arbiol, S. Estradé, F. Peirò, J. R. Morante, and M. Eickhoff, J. Appl. Phys. **104**, 034309 (2008).
[24]R. Armitage and K. Tsubaki, Nanotechnology **21**, 195202 (2010).
[25]C. Chèze, L. Geelhaar, O. Brandt, W. M. Weber, H. Riechert, S. Münch, R. Rothemund, S. Reitzenstein, A. Forchel, T. Kehagias, P. Komniou, G. P. Dimitrakopulos, and T. Karakostas, Nano Res. **3**, 528 (2010).
[26]S. Nishikawa and K. Matsukawa, Proc. Imp. Acad. Jpn. **4**, 96 (1928).
[27]D. Coster, K. S. Knol, and J. A. Prins, Z. Phys. **63**, 345 (1930).
[28]A. W. Stevenson, S. W. Wilkins, M. S. Kwietniak, and G. N. Pain, J. Appl. Phys. **66**, 4198 (1989).
[29]R. D. Horning and B. L. Goldenberg, Appl. Phys. Lett. **55**, 1721 (1989).
[30]D. C. Meyer, K. Richter, H.-G. Krane, W. Morgenroth, and P. Paufler, J. Appl. Cryst. **32**, 854 (1999).
[31]H. Tampo, P. Fons, A. Yamada, K.-K. Kim, H. Shibata, K. Matsubara, and S. Niki, Appl. Phys. Lett. **87**, 141904 (2005).
[32]J. Als-Nielsen and D. McMorrow, *Elements of Modern x-Ray Physics* (Wiley, Chichester, UK, 2001), Chap. 7, Sec. 5.
[33]J.-L. Hodeau, V. Favre-Nicolin, S. Bos, H. Renevier, E. Lorenzo, and J.-F. Berar, Chem. Rev. **101**, 1843 (2001).
[34]H. Renevier, S. Grenier, S. Arnaud, J. F. Bérar, B. Caillot, J. L. Hodeau, A. Letoublon, M. G. Proietti, and B. Ravel, J. Synchrotron Radiat. **10**, 435 (2003).
[35]D. Waasmaier and A. Kirfel, Acta Crystallogr. Sect. A **51**, 416 (1995).
[36]S. Sasaki, KEK Report **88-14**, 1 (1989).
[37]J. O. Cross, M. Newville, J. J. Rehr, L. B. Sorensen, C. E. Bouldin, G. Watson, T. Gouder, G. H. Lander, and M. I. Bell, Phys. Rev. B. **58**, 11215 (1998).
[38]Z. T. Wang, Y. Yamada-Takamura, Y. Fujikawa, T. Sakurai, and Q. K. Xue, Appl. Phys. Lett. **87**, 032110 (2005).
[39]M. K. Sunkara, S. Sharma, R. Miranda, G. Lian, and E. C. Dickey, Appl. Phys. Lett. **87**, 1546 (2001).
[40]E. Calleja, J. Ristic, S. Fernandez-Garrido, L. Cerutti, M. A. Sanchez-Garcia, J. Grandal, A. Trampert, U. Jahn, G. Sanchez, A. Griol, and B. Sanchez, Phys. Status Solidi B **244**, 2816 (2007).
[41]G. Radtke, M. Couillard, G. A. Botton, D. Zhu, and C. J. Humphreys, Appl. Phys. Lett. **97**, 251901 (2010).
[42]O. Landré, C. Bougerol, H. Renevier, and B. Daudin, Nanotechnology **20**, 415602 (2009).
[43]H. Sekiguchi, T. Nakazato, A. Kikuchi, and K. Kishino, J. Cryst. Growth **300**, 259 (2007).
[44]O. Landré, R. Songmuang, J. Renard, E. Bellet-Amalric, H. Renevier, and B. Daudin, Appl. Phys. Lett. **93**, 183109 (2008).
[45]L. Largeau, D. L. Dheeraj, M. Tchernycheva, G. E. Cirlin, and J. C. Harmand, Nanotechnology **19**, 155704 (2008).
[46]A. Bourret, A. Barski, J. L. Rouvière, G. Renaud, and A. Barbier, J. Appl. Phys. **83**, 2003 (1998).